

Towards a comprehensive database to study the impact of image quality on abnormality detection and classification in Wireless Capsule Endoscopy

Tan Sy NGUYEN

tansy.nguyen@math.univ-paris13.fr

LAGA, L2TI
Université Sorbonne Paris Nord

October 15, 2021



Overview

1 Motivation & Context

- Context
- Wireless Capsule Endoscopy
 - Challenges
 - Solutions

2 Existing datasets

- Existing GI datasets
- HyperKvasir dataset

3 Our work

- Method
- Results

Context

Example

In 2018, the Colorectal cancer (CRC) is the third (second respectively) leading cause of cancer death in the world (France, respectively).^{1,2}

¹ Bray F, Ferlay J, Soerjomataram I, Siegel RL, Torre LA, Jemal A, "Global cancer statistics 2018: GLOBOCAN estimates of incidence and mortality worldwide for 36 cancers in 185 countries", CA Cancer J Clin. 2018 Nov; 68(6):394-424.

² Faivre J, Dancourt V, et. al, Santé Publique France, "Cancer du colon rectum", <https://www.santepubliquefrance.fr/maladies-et-traumatismes/cancers/cancer-du-colon-rectum>

³ McKESSON, "Colorectal Cancer & Laboratory Screening", 2018



Context

Example

In 2018, the Colorectal cancer (CRC) is the third (second respectively) leading cause of cancer death in the world (France, respectively).^{1,2}

Solution

Studies have shown that early detection can result in up to a **92% survival rate for stage I of cancer.**³

¹ Bray F, Ferlay J, Soerjomataram I, Siegel RL, Torre LA, Jemal A, "Global cancer statistics 2018: GLOBOCAN estimates of incidence and mortality worldwide for 36 cancers in 185 countries", CA Cancer J Clin. 2018 Nov; 68(6):394-424.

² Faivre J, Dancourt V, et. al, Santé Publique France, "Cancer du colon rectum", <https://www.santepubliquefrance.fr/maladies-et-traumatismes/cancers/cancer-du-colon-rectum>

³ McKESSON, "Colorectal Cancer & Laboratory Screening", 2018

Effect of distortion (Blur) on the classification performance ⁵

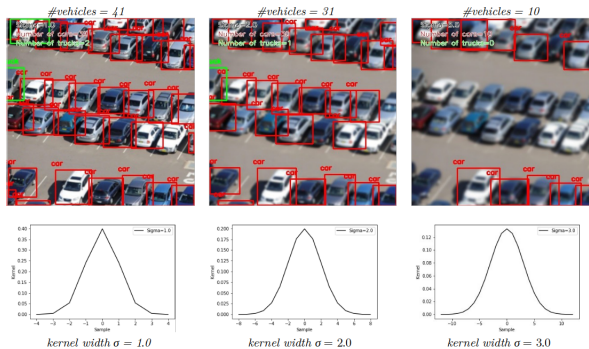


Figure 3: Degradation of the vehicle detection due to image blurring. Left column: Blurred image with kernel width $\sigma = 1.0$ detects 41 vehicles. Middle column: Blurred image with kernel width $\sigma = 2.0$ detects 31 vehicles. Right column: Blurred image with kernel width $\sigma = 3.0$ detects 10 vehicles.

⁵

Borel-Donohue, Christoph and S. Young. "Image quality and super resolution effects on object recognition using deep neural networks." Defense + Commercial Sensing (2019).

How we can handle the distortions to enhance the image quality; therefore, improve the classification performance?



Method

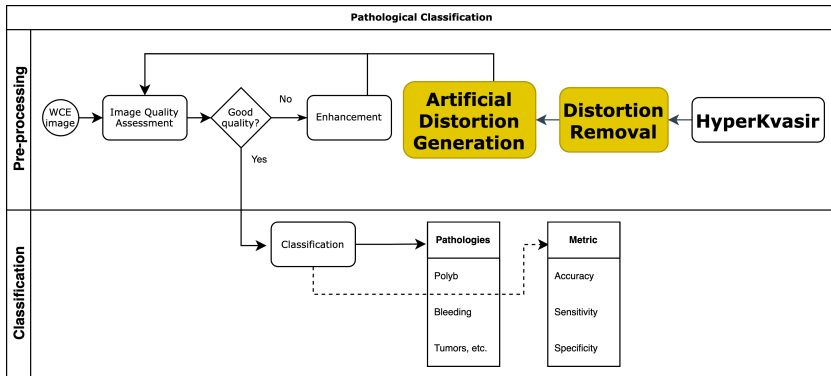


Figure 7: Flow chart of the pathological classification process

Existing datasets

Table 1: An overview of existing GI datasets.

Dataset	Findings	Size
CVC-356 [1]	Polyps	356 images
CVC-ClinicDB (also named CVC-612) [2]	Polyps	612 images
CVC-VideoClinicDB (also named CVC-12k) [1]	Polyps	11954 images
CVC-ColonDB [1]	Polyps	380 images
Endoscopy Artifact detection 2019 [3]	Endoscopic Artifacts	5,138 images
ASU-Mayo polyp database [4]	Polyps	18,781 images
ETIS-Larib Polyp DB [5]	Polyps	196 images
KID [6]	Angiectasia, bleeding, inflammations, polyps	2371 images and 47 videos
GIANA 2017 [7]	Polyps & Angiodysplasia	3462 images and 38 videos
GIANA 2018 [8]	Polyps & Small bowel lesions	8262 images and 38 videos
GASTROLAB [9]	GI lesions	Some 100s of images and few videos
WEO Clinical Endoscopy Atlas [10]	GI lesions	152 images
GI Lesions in Regular Colonoscopy Data Set [11]	GI lesions	76 images
Atlas of Gastrointestinal Endoscopy [12]	GI lesions	1295 images
EI salvador atlas of gastrointestinal video endoscopy [13]	GI lesions	5071 video clips
Kvasir [14]	Polyps, esophagitis, ulcerative colitis, Z-line, pylorus cecum, dyed polyp, dyed resection margins, stool	8000 images
Kvasir-SEG [15]	Polyps	1000 images
Nerthus [16]	Stool - categorization of bowel cleanliness	21 videos

Existing datasets

Table 1: An overview of existing GI datasets.

Dataset	Findings	Size
CVC-356 [1]	Polyps	356 images
CVC-ClinicDB (also named CVC-612) [2]	Polyps	612 images
CVC-VideoClinicDB (also named CVC-12k) [1]	Polyps	11954 images
CVC-ColonDB [1]	Polyps	380 images
Endoscopy Artifact detection 2019 [3]	Endoscopic Artifacts	5,138 images
ASU-Mayo polyp database [4]	Polyps	18,781 images
ETIS-Larib Polyp DB [5]	Polyps	196 images
KID [6]	Angiectasia, bleeding, inflammations, polyps	2371 images and 47 videos
GIANA 2017 [7]	Polyps & Angiodysplasia	3462 images and 38 videos
GIANA 2018 [8]	Polyps & Small bowel lesions	8262 images and 38 videos
GASTROLAB [9]	GI lesions	Some 100s of images and few videos
WEO Clinical Endoscopy Atlas [10]	GI lesions	152 images
GI Lesions in Regular Colonoscopy Data Set [11]	GI lesions	76 images
Atlas of Gastrointestinal Endoscope [12]	GI lesions	1295 images
EI salvador atlas of gastrointestinal video endoscopy [13]	GI lesions	5071 video clips
Kvasir [14]	Polyps, esophagitis, ulcerative colitis, Z-line,pylorus cecum, dyed polyp, dyed resection margins, stool	8000 images
Kvasir-SEG [15]	Polyps	1000 images
Nerthus [16]	Stool - categorization of bowel cleanliness	21 videos

They are rather small, and often limited to polyps. Several of these have also lately become unavailable.



Existing datasets

Table 1: An overview of existing GI datasets.

Dataset	Findings	Size
CVC-355 [1]	Polyps	356 images
CVC-ClinicDB (also named CVC-612) [2]	Polyps	612 images
CVC-VideoClinicDB (also named CVC-12k) [1]	Polyps	11954 images
CVC-ColonDB [1]	Polyps	380 images
Endoscopy Artifact detection 2019 [3]	Endoscopic Artifacts	5,138 images
ASU-Mayo polyp database [4]	Polyps	18,781 images
ETIS-Larib Polyp DB [5]	Polyps	196 images
KID [6]	Angiectasia, bleeding, inflammations, polyps	2371 images and 47 videos
GIANA 2017 [7]	Polyps & Angiodysplasia	3462 images and 38 videos
GIANA 2018 [8]	Polyps & Small bowel lesions	8262 images and 38 videos
GASTROLAB [9]	GI lesions	Some 100s of images and few videos
WEO Clinical Endoscopy Atlas [10]	GI lesions	152 images
GI Lesions in Regular Colonoscopy Data Set [11]	GI lesions	76 images
Atlas of Gastrointestinal Endoscope [12]	GI lesions	1295 images
EI salvador atlas of gastrointestinal video endoscopy [13]	GI lesions	5071 video clips
Kvasir [14]	Polyps, esophagitis, ulcerative colitis, Z-line,pylorus cecum, dyed polyp, dyed resection margins, stool	8000 images
Kvasir-SEG [15]	Polyps	1000 images
Nerthus [16]	Stool - categorization of bowel cleanliness	21 videos

They are rather small, and often limited to polyps. Several of these have also lately become unavailable.

Using **HyperKvasir** [17] dataset



HyperKvasir dataset

Table 2: Overview of the data records in the HyperKvasir dataset.

Data Record	# Files	Description
Labeled images	10,662 images	23 classes of findings
Segmented Images	1,000 images	Segmentation masks for polyp findings
Unlabeled Images	99,417 images	Unlabeled
Videos	374 videos	30 different classes

HyperKvasir dataset

Table 2: Overview of the data records in the HyperKvasir dataset.

Data Record	# Files	Description
Labeled images	10,662 images	23 classes of findings
Segmented Images	1,000 images	Segmentation masks for polyp findings
Unlabeled Images	99,417 images	Unlabeled
Videos	374 videos	30 different classes



Figure 8: Image examples of the various labeled classes for images and/or videos.

Our work

Our work has three stages including:

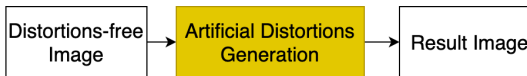
- 1 Remove the existing distortion in HyperKvasir dataset
- 2 Create the model to generate the new artificial distortions
- 3 Add the new artificial distortions to the distortions-free images.



1 Remove the existing distortions



2 Create the artificial distortions model



3 Add the artificial distortions to the distortions-free image

1. Remove the existing distortion in HyperKvasir dataset

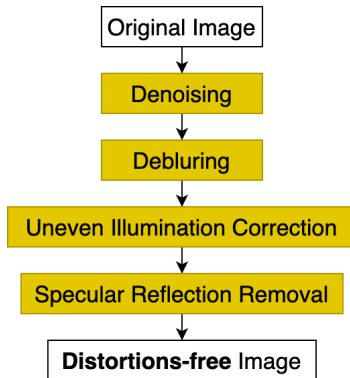
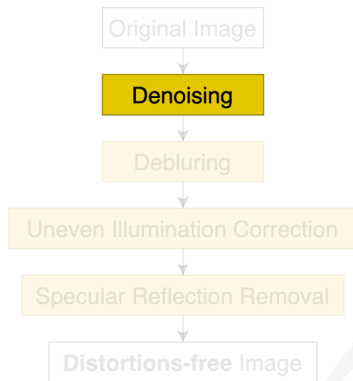


Figure 9: Process to remove the existing distortion in HyperKvasir dataset. The original image will go through four enhancement blocks corresponding to four common distortions: Noise, Blur, Uneven Illumination and Specular Reflection.

1.1 Denoising



Noise standard deviation estimation

For an image I with width W and height H , the estimated standard deviation σ_n of noise is estimated as⁸:

$$\sigma_n = \sqrt{\frac{\pi}{2} \frac{1}{6(W-2)(H-2)} \sum_{x,y} |I(x, y) * M_N|} \quad (1)$$

where $M_N = 2(L_2 - L_1)$ with the given L_1, L_2 :

$$L_1 = \begin{bmatrix} 0 & 1 & 0 \\ 1 & -4 & 1 \\ 0 & 1 & 0 \end{bmatrix} \quad (2)$$

$$L_2 = \begin{bmatrix} 1 & 0 & 1 \\ 0 & -4 & 0 \\ 1 & 0 & 1 \end{bmatrix} \quad (3)$$

⁸Immerkær, John. "Fast Noise Variance Estimation." *Comput. Vis. Image Underst.* 64 (1996): 300-302.

Autoencoder used for denoising

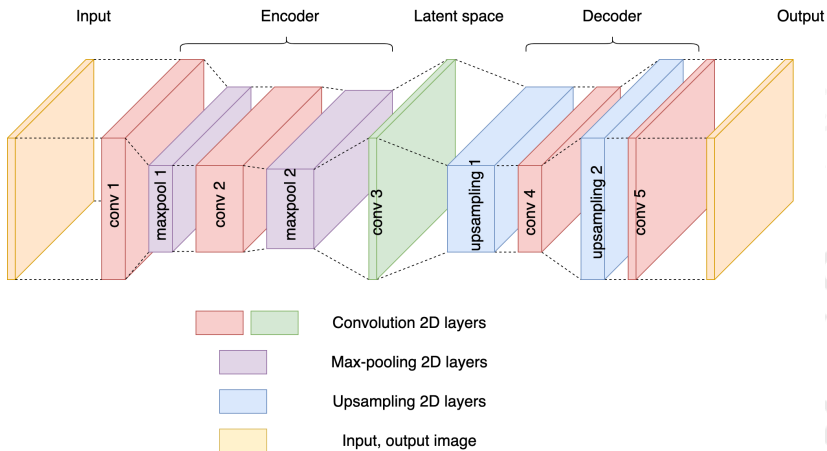


Figure 10: The Autoencoder model used for denoising

Results on Image denoising

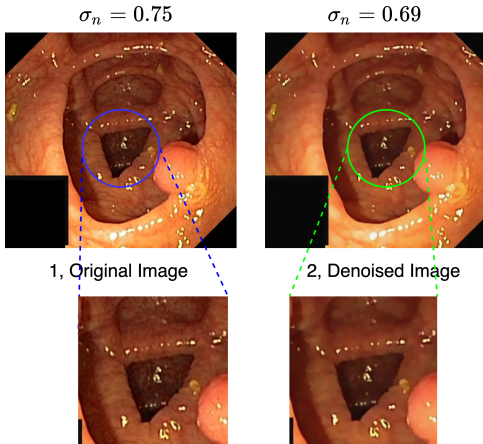
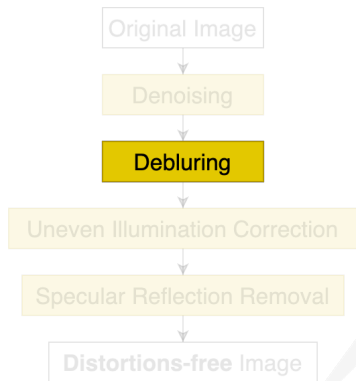


Figure 11: The results of the denoising experiment. The estimated noise standard deviation after denoising has been decreased showing the effectiveness of denoising method.

1.2 Debluring



Blurring index to estimate the level of blur

Apply the **variance of the Laplacian**⁹[18] method to your own images to detect the amount of blurring.

$$\text{index}_b = \text{var}(\mathcal{L}(f(x, y))), \quad (4)$$

where $f(x, y)$ is the input image



⁹Pertuz, Said et al. "Analysis of focus measure operators for shape-from-focus." Pattern Recognit. 46 (2013): 1415-1432.

DeblurGAN-v2¹⁰ model for deblurring

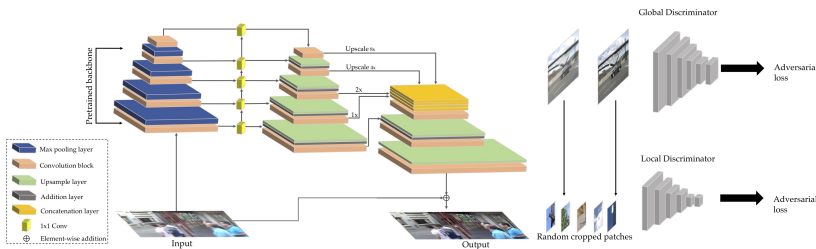


Figure 12: The DeblurGAN v2 model used for deblurring [19]

¹⁰ Kupyn, Orest et al. "DeblurGAN-v2: Deblurring (Orders-of-Magnitude) Faster and Better." 2019 IEEE/CVF International Conference on Computer Vision (ICCV) (2019): 8877-8886.

Results on image deblurring

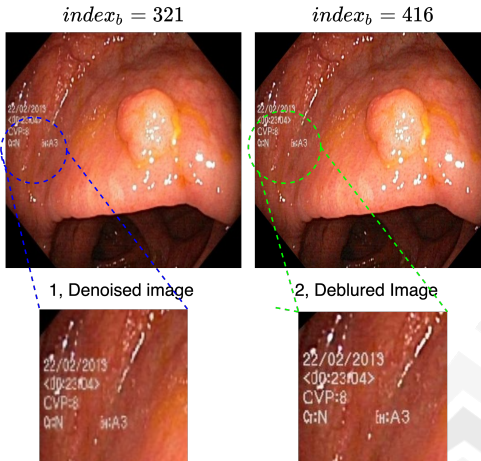
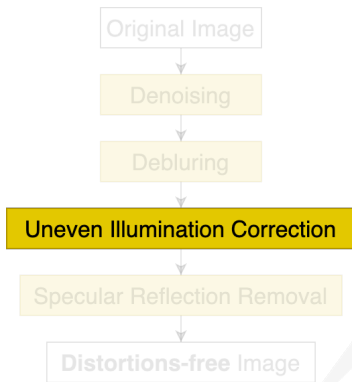


Figure 13: The deblurred result. The Laplacian index after deblurring has been increased. The region of number shows clearly effectiveness of deblurring method.

1.3 Uneven Illumination Correction



Uneven Illumination correction¹¹ process

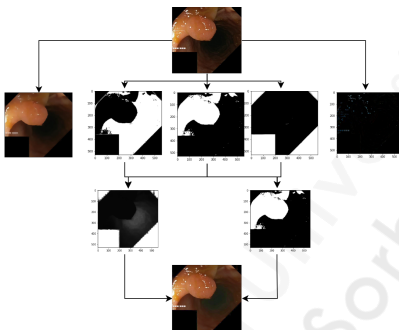
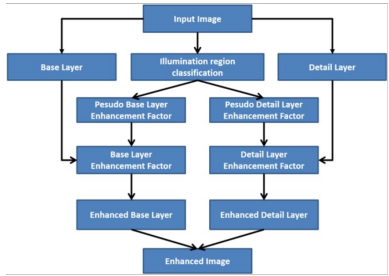


Figure 14: Uneven Illumination Correction process using [20]

¹¹ Xia, Wenyao et al. "Endoscopic image enhancement with noise suppression." Healthcare Technology Letters 5 (2018): 154 - 157.

Results on Uneven Illumination Correction

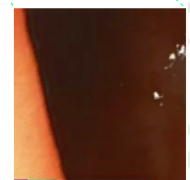
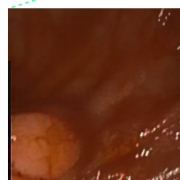
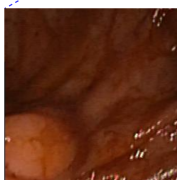
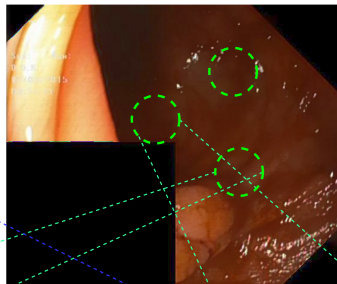
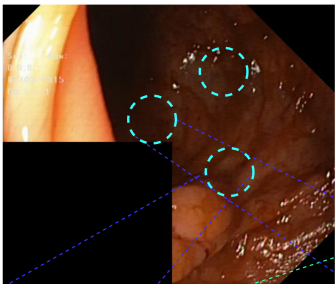
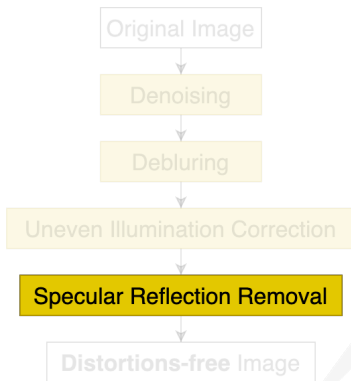


Figure 15: Uneven Illumination Correction result. The first row is the original image with some uneven illumination region (cyan circle). In the second column, these regions have been corrected (green circle)

1.3 Specular Reflection Removal



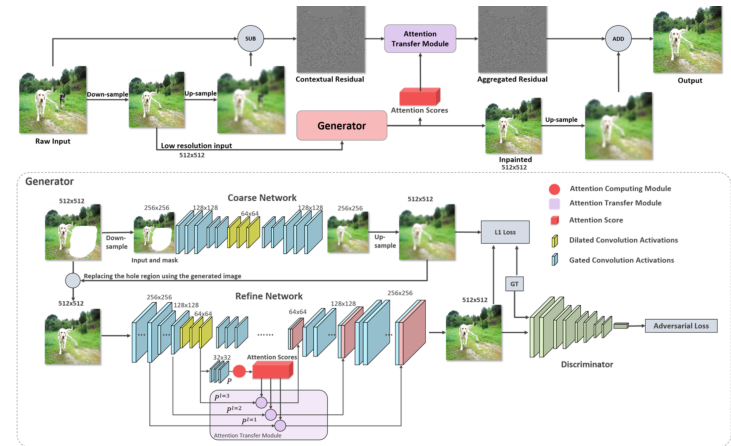
Specular Reflection removal¹²

Figure 16: The overall pipeline of the method: (top) Contextual Residual Aggregation (CRA) mechanism, (bottom) the architecture of the generator [21]

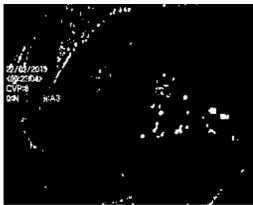
¹²

Yi, Zili et al. "Contextual Residual Aggregation for Ultra High-Resolution Image Inpainting." 2020 IEEE/CVF Conference on Computer Vision and Pattern Recognition (CVPR) (2020): 7505-7514.

Results on Specular Reflection Removal



Original Image



Specular Reflection Mask

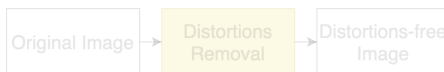


Result

Figure 17: Specular Reflection Removal result. First columns: the input image with specular references. The third column is the result of the Specular Reflection inpainted image using the SR mask (second column) inspired from [22].

2. Create model and add the artificial distortions to the distortions-free images

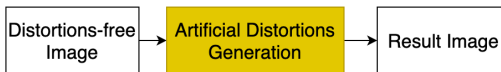
In this work, we create a model to add the artificial distortion to the image. There will be **four** different models corresponding to four kinds of distortions. We analysed the common level of distortion to simulate to realest artificial distortion which will make the dataset meaningful.



1 Remove the existing distortions



2 Create the artificial distortions model



3 Add the artificial distortions to the distortions-free image



2.1 Result images after adding Noise



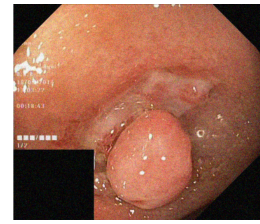
AWGN kernel width

$$\sigma_n = 0.01$$

$$\hat{I} = I + n$$

where n is the noise whose distribution

$$N(0, \sigma_n^2)$$



AWGN kernel width

$$\sigma_n = 0.1$$

Figure 18: Noising image with Gaussian Noise $n \sim N(0, \sigma_n^2)$

2.2 Result images after adding Blur



Defocus blur kernel width

$$\sigma_{db} = 2$$



Motion blur kernel width of PSF

$$l_{mb} = 20$$

Figure 19: Bluring image with Defocus Blur $b \sim N(0, \sigma_{db}^2)$ and motion blur PSF kernel width l_{mb}

2.3 Result images after adding Uneven Illumination

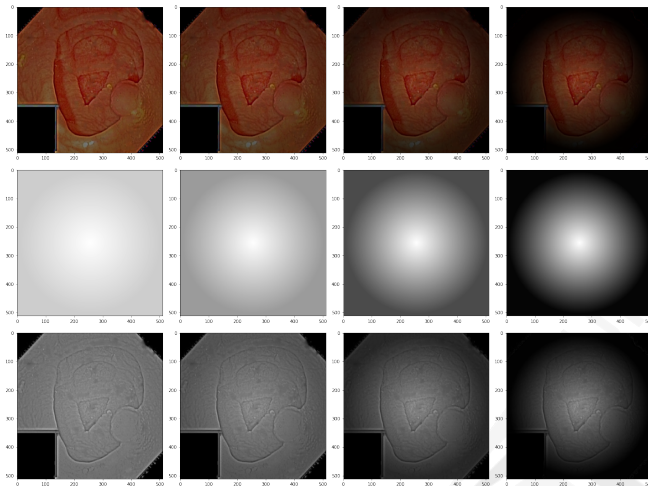
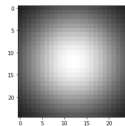


Figure 20: Artificial Uneven Illumination process. The first row is the result after adding the mask (second row) into the V-channel of image (third row).

2.4 Result images after adding Specular Reflection



Input image



Artificial SR point spread function



Output Image

Figure 21: Artificial Specular Reflection by using the artificial PSF with the random position

References

- [1] Jorge Bernal, F. J. Sánchez, and F. Vilariño. "Towards automatic polyp detection with a polyp appearance model". In: **Pattern Recognit.** 45 (2012), pp. 3166–3182.
- [2] Jorge Bernal et al. "WM-DOVA maps for accurate polyp highlighting in colonoscopy: Validation vs. saliency maps from physicians". In: **Computerized medical imaging and graphics : the official journal of the Computerized Medical Imaging Society** 43 (2019), pp. 99–111.
- [3] Sharib Ali et al. "Endoscopy artifact detection (EAD 2019) challenge dataset". In: **ArXiv** abs/1905.03209 (2019).
- [4] Nima Tajbakhsh, S. Gurudu, and Jianming Liang. "Automated Polyp Detection in Colonoscopy Videos Using Shape and Context Information". In: **IEEE Transactions on Medical Imaging** 35 (2016), pp. 630–644.
- [5] Juan Silva et al. "Toward embedded detection of polyps in WCE images for early diagnosis of colorectal cancer". In: **International Journal of Computer Assisted Radiology and Surgery** 9 (2013), pp. 283–293.
- [6] A. Koulaouzidis et al. "KID Project: an internet-based digital video atlas of capsule endoscopy for research purposes". In: **Endoscopy International Open** 5 (2017), E477–E483.
- [7] Y. Guo and B. Matuszewski. "GIANA Polyp Segmentation with Fully Convolutional Dilated Neural Networks". In: **VISIGRAPP** (2019).
- [8] Jorge Bernal et al. "Polyp Detection Benchmark in Colonoscopy Videos using GTCreator: A Novel Fully Configurable Tool for Easy and Fast Annotation of Image Databases". In: (2018).
- [9] the gastrointestinal site. "Gastrolab". In: <http://www.gastrolab.net/index.htm>. Accessed: 2019-12-12 (2019).
- [10] Endoatlas. "Weo clinical endoscopy atlas". In: <http://www.endoatlas.org/index.php>. Accessed: 2019-12-12 (2019).
- [11] UCI. "Gastrointestinal lesions in regular colonoscopy dataset". In: (2019). URL: http://www.depeca.uah.es/colonoscopy_dataset/.
- [12] Atlas. "The atlas of gastrointestinal endoscopy". In: (2019). URL: http://www.endoatlas.com/atlas_1.html.
- [13] Atlas. "El salvador atlas of gastrointestinal video endoscopy". In: (2019). URL: <http://www.gastrointestinalatlas.com/index.html>.
- [14] Konstantin Pogorelov et al. "KVASIR: A Multi-Class Image Dataset for Computer Aided Gastrointestinal Disease Detection". In: **Proceedings of the 8th ACM on Multimedia Systems Conference** (2017).
- [15] Debeh Jha et al. "Kvasir-SEG: A Segmented Polyp Dataset". In: **ArXiv** abs/1911.07069 (2020).
- [16] Konstantin Pogorelov et al. "Nerthus: A Bowel Preparation Quality Video Dataset". In: **Proceedings of the 8th ACM on Multimedia Systems Conference** (2017).
- [17] Hanna Borgli et al. "HyperKvasir, a comprehensive multi-class image and video dataset for gastrointestinal endoscopy". In: **Scientific Data** 7 (2020).
- [18] Saïd Pertuz, Domenec Puig, and Miguel Ángel García. "Analysis of focus measure operators for shape-from-focus". In: **Pattern Recognit.** 46 (2013), pp. 1415–1432.
- [19] Orest Kupyn et al. "DeblurGAN-v2: Deblurring (Orders-of-Magnitude) Faster and Better". In: **2019 IEEE/CVF International Conference on Computer Vision (ICCV)** (2019), pp. 8877–8886.
- [20] Wenyao Xia, Elvis C. S. Chen, and Terry M. Peters. "Endoscopic image enhancement with noise suppression". In: **Healthcare Technology Letters** 5 (2018), pp. 154–157.
- [21] Zili Yi et al. "Contextual Residual Aggregation for Ultra High-Resolution Image Inpainting". In: **2020 IEEE/CVF Conference on Computer Vision and Pattern Recognition (CVPR)** (2020), pp. 7505–7514.
- [22] Zili Yi et al. "Contextual Residual Aggregation for Ultra High-Resolution Image Inpainting". In: **Proceedings of the IEEE/CVF Conference on Computer Vision and Pattern Recognition** (2020), pp. 7508–7517.

Thank you for watching!

Contact:

tansy.nguyen@math.univ-paris13.fr

